

Identification of Prognostic Alternative Splicing Signature in Gastric Cancer

Zhiwu Wang

Tangshan People's Hospital

Qiong Wu

Tangshan People's Hospital

Yankun Liu

Tangshan People's Hospital

Jingwu Li (✉ tssrmyy_ljw@163.com)

Tangshan People's Hospital

Research Article

Keywords: gastric cancer, prognosis, aberrant alternative splicing, bioinformatic analysis

Posted Date: February 12th, 2021

DOI: <https://doi.org/10.21203/rs.3.rs-183022/v1>

License: © ⓘ This work is licensed under a Creative Commons Attribution 4.0 International License.

[Read Full License](#)

Abstract

Aberrant alternative splicing (AS) events serve as prognostic indicators in a large number of malignancies, whereas comprehensive analysis of prognostic AS in gastric cancer (GC) has not yet been understood. To identify prognostic AS events and clarify the function of the splicing variants in GC. RNA-Seq data, clinical information and percent spliced in (PSI) values were available in the cancer genome atlas (TCGA) and TCGA SpliceSeq data portal. A three-step regression method was conducted to screen prognostic AS events and construct multi-AS-based signatures. The associations between prognostic AS events and splicing factors were also investigated. We identified a total of 1318 survival related AS events in GC, Parent genes of which were implicated in numerous oncogenic pathways. The final prognostic signatures stratified by seven types of AS events or not stratified performed well in risk prediction for GC patients. Moreover, five signatures base on AA, AD, AT, ES and RI events function as independent prognostic indicators after multivariate adjustment of clinical/pathological variables. Splicing network also showed marked correlation between the expression of splicing factors and PSI value of AS events in GC patients. The AS derived signatures allow to predict GC prognosis and might serve as potential therapeutic target for GC.

Introduction

Gastric cancer (GC) remains the public health burden worldwide with high morbidity and mortality, and there are estimated 27,600 new diagnosed cases and 11,010 GC-related deaths in 2018¹. A majority of patients were diagnosed at an advanced stage, missing the optimal opportunity of surgical resection, and thus had the dismal prognosis with the overall 5 year survival rate of 32.0%¹. Therefore, better understanding of the mechanism of GC contributes to develop effective strategies of early diagnosis, prognosis prediction and even therapy.

Alternative splicing (AS) is a post-transcriptional regulatory mechanism by which differential splicing of exons occurs, resulting in the diversity of mRNAs and proteins. Over 95% of human genes undergo AS and encode splicing variants with different or even opposite functions². Differential splicing of the same pre-mRNA generates mature isoforms and proteins with different structures and functions. Under normal circumstances, AS is essential for complex biological behaviors. Once disordered, however, abnormal protein isoforms with inserted, missing or altered function domains may drive or promote oncogenic processes. Moreover, it has been widely acknowledged that AS events are closely associated with gastric carcinogenesis and progression^{3,4}.

Tumor development is a multi-step, multi-factor processes. Thus, constructing a risk prediction model consisting of diverse biomarkers is an effective and reliable strategy compared to using a single clinicopathological indicator. To improve the predictive accuracy for malignancies including GC, numerous studies had built diverse prognostic models using several mRNAs, miRNAs and long non-coding RNAs based on transcriptome-wide profiles⁵⁻⁷. Although the mechanism of AS events is complicated and remains poorly understood to some extent, their prognostic role has been emphasized in

a large number of cancers⁸⁻¹². Considering the role of AS in GC, there is an urgent need to build the prediction model of AS events and screen high-risk patients with GC.

Results

Overview of AS events and related genes in GC cohort

AS events could be divided into seven types as illustrated in Fig.1A, including Exon skip (ES), Alternate promoter (AP), Alternate terminator (AT), Mutually exclusive exons (ME), Retained intron (RI), Alternate acceptor site (AA) and Alternate donor site (AD). Through strict filtering, 19698 AS events from 11579 parent genes were identified in 364 GC patients, including 7189 ESs in 3562 genes, 4310 APs in 2474 genes, 3487 ATs in 1979 genes, 1664 AAs in 1310 genes, 1542 ADs in 1174 genes, 1391 RIs in 985 genes and 106 MEs in 104 genes (Fig.1B). In addition, the Upset plot indicated that one gene possesses several types of AS events (Fig.1C).

Identification of survival related AS events in GC cohort

Through Univariate Cox regression analysis, a total of 1318 AS events from 957 parent genes were viewed as prognostic ones, including 464 ESs in 377 genes, 352 APs in 229 genes, 200 ATs in 133 genes, 79 AAs in 79 genes, 128 ADs in 121 genes, 81 RIs in 75 genes and 14 MEs in 14 genes (Fig.1B). Moreover, intersections among these seven types of AS events were exhibited with the Upset plot (Fig.1D), demonstrating that one gene could hold up to several types of prognostic AS events.

Bioinformatics analysis of survival associated AS events

To elucidate the potential interference of OS associated AS events and corresponding proteins, 957 parent genes of 1391 AS events were sent for bioinformatics analyses, including GO (Gene Ontology), KEGG (Kyoto Encyclopedia of Genes and Genomes) and PPI (Protein-Protein Interaction). As a result, 4 terms in biological process, 8 terms in cellular component and 10 terms in molecular function were highlighted via GO analysis (Fig.2A). Moreover, 11 of 23 remarkably enriched KEGG pathways seem to be implicated in oncogenic processes, including Basal cell carcinoma, Autophagy, Proteoglycans in cancer, ECM-receptor interaction, Gastric cancer, Hepatocellular carcinoma, Focal adhesion, EGFR tyrosine kinase inhibitor resistance, Cell cycle, HIF-1 signaling pathway and Wnt signaling pathway (Fig.2B). To further explore the significances of these parent genes, a PPI network was constructed which incorporated 373 nodes and 960 edges (Fig.2C). Moreover, the key module, composed of 25 nodes and 297 edges, was processed via CytoHubba tool (Fig.2D). The parent genes/proteins in the key module were mainly comprised of ribosomal proteins (RPS5, RPS6, RPLP0, etc) and ribonucleoproteins (HNRNPC, HNRNPR, SNRNP70, etc).

Construction of the prognostic signature using AS events for GC patients

To minimize the counts of the prognostic model, lasso and multivariate Cox regression methods were performed. After lasso regression filtering, 20 variables (If available) in each splicing type dropped to 20 in AA, 19 in AD, 17 in AP, 16 in AT, 17 in ES, 13 in ME, 15 in RI and 17 in all types, respectively (Fig.3A-H). Then, the selected AS events were further screened by the multivariate Cox regression, and thus final prognostic models were constructed, containing 15 AA, 14 AD, 9 AP, 10 AT, 13 ES, 8 ME, 10 RI and 11 mixed events, respectively (Fig.4A-H).

Using the median value of the riskscore as the cutoff, GC patients were classified into high- and low- risk groups. The Kaplan-Meier curves were employed to demonstrate the survival variation of patients between these two groups. Each AS-based prognostic model, stratified by AA, AD, AP, AT, ES, ME, RI events or not stratified, indicated the predictive power that patients in the high-risk group had poorer OS than those in the low-risk group, respectively (Fig.5A-H).

ROC curves were generated to assess the predictive accuracy of the eight AS prognostic models. As illustrated in Fig.5I, the risk score of AD model showed the greatest predictive power with an AUC of 0.804, followed by AA, AP, AT, RI and the model not stratified by AS types. The performance of these prognostic signatures with AUC>0.7 were further tested in predicting the survival status. With the increasing risk score calculated by any type of AUC>0.7 (AA, AD, AP, AT, RI and mixed events), there were more patients dead and less patients living, respectively (Fig.6A-F).

To determine whether the final model was an independent prognostic factor for GC, AS predictive models along with age, gender, grade and clinical stage, were once again sent for Uni/Multivariate Cox regression analysis. Although AA, AD, AP, AT, ES, ME, RI and mixed events exhibited predictive performance (Fig. 7A), risk scores calculated by the formula of AA, AD, AT, ES, RI events were independent prognostic indicators (Fig.7B).

Interactive analysis of Splicing factors and AS events

The regulatory network was built based on the expression of SF genes and PSI values of AS events via using the cytoscape software. As shown in Fig.8A, prognostic AS events, including 20 risky (red node) and 14 favorable ones (green node), were positively or negatively modulated by the key SF genes (blue node). Remarkably, the same SF could regulate different AS events, and the same AS could be regulated by different SFs. Moreover, a majority of adverse AS events were positively associated with SFs (red line), whereas most favorable AS events were negatively associated with SFs (green line). For the same gene and same splicing type, the SF may play different or even opposite roles producing different isoforms. For example, QKI expression was positively correlated with AT event of SEPT11-69618, but negatively correlated with AT event of SEPT11-69616 (Fig.8B, C).

Discussion

Through AS, differential proteins with differential structures and functions can be generated and may be associated with carcinogenesis. Thus, alternative spliced isoforms and AS events could be served as

diagnostic, predictive, prognostic biomarkers and even therapeutic target in a large number of cancers¹³⁻¹⁶. Recent studies demonstrated that Aberrant AS events inducing-variants affected important phenotypes of GC, including proliferation, apoptosis, metastasis and chemotherapy resistance¹⁷⁻¹⁹. Currently, Chuan Liu et al²⁰ and Victoria E S Armero et al²¹ had determined the prediction model of AS events in *Helicobacter pylori*-negative cohort and *Epstein-Barr* virus cohort of GC, respectively. However, the present study depicted the landscape of AS profiles within the entire GC cohort and respectively constructed the risk prediction model stratified by 7 types of AS. In addition, a series of GC-specific and survival associated AS events as well as SFs were identified, which would provide potential intervention targets for GC therapy.

Alternative splicing is one of the critical mechanisms by which the diversity of mRNAs and corresponding proteins occurs in organism. In the present study, a total of 19698 AS events of 11579 genes were detected, showing that AS is a common process in GC and one gene generates several transcripts. Next, we identified 1318 prognosis related AS events of 957 genes. To explore how these AS events drive tumor initiation, the parent genes were incorporated into GO and KEGG pathway enrichment analyses. These spliced genes were closely associated with HIF-1/Wnt/ErbB/p53 oncogenic pathways. Moreover, we established a PPI network and obtained a key module consisting of 40 hub genes, including splicing factors and ribosomal proteins.

To minimize the number of prognosis related AS events of the prediction model, we further performed the stepwise lasso and multivariate Cox regressions. Ultimately, seven risk prediction models stratified by AS types as well as one non-stratified prediction model were constructed, respectively. Although prognostic AS signatures of GC had been produced in Zhen Zong et al and *ZhangSetal*s reports^{22,23}, our screening strategy seems more reasonable. We first identified OS related AS events through Univariate Cox and lasso regression methods, followed by Multivariate Cox regression analysis. Conversely, lasso regression analysis was not employed in Zhen Zong et al *srep* or *t*, and *MtivariateC* \otimes *regressionmethodswas* \neg *used* \in *ZhangSetal*s report. The

inadequacy of statistical strategy may lead to the overfitting of the risk model and affect the predictive performance of the model.

Importantly, AD showed the most reliable predictive capacity among AS events with the AUC value of 0.804, followed by AA event. Unparalleled with our study, AA event exhibited the highest AUC value, followed by AD event in Zong S et al's report. The distinction may arise from the screening strategy of OS related AS events mentioned above. The AUC > 0.8 is generally considered to be adequate for clinics, so AD event should be highlighted excessively for prospects of clinical application. In addition, via Cox regression analysis with other clinical parameters, AD event was proved to be an independent prognostic indicator of GC. Within the prediction model of AD events, two genes (HY1, FBXW2) were adverse and the other 12 were favorable factors of GC. As the critical E3 ubiquitin ligase, FBXW2 retards tumor proliferation and metastasis via degrading tumor-associated transcription factors or coactivators²⁴.

However, if FBXW2 is spliced by AD event, it becomes a poor prognostic indicator which may facilitate tumorigenesis and progression of GC.

Mutations or alterations in the expression of regulatory splicing factors could cause aberrant AS events and production of differential spliced variants, thus promoting or inhibiting the oncogenic phenotype in multiple cancers^{25,26}. By constructing the regulatory network between the expression of SFs and PSI value of OS related AS events, we identified 16 critical SFs, some of which had been documented to exhibit pro-oncogenic or anti-oncogenic behavior in a series of malignancies, including GC. These SFs regulate the expression of the spliced variants derived from the same pre-mRNA via different AS events. Even within the same gene, the same AS event in multiple loci may generate differential spliced variants with the same or opposite behavior. For instance, QKI served as a tumor suppressor and inhibited gastric carcinogenesis via alternative splicing of the histone macroH2A1²⁷. In our bioinformatics analysis, QKI may play a dual role in the development of GC, promoting tumorigenesis via a poor prognostic AS indicator (Fig. 3B) or inhibiting tumorigenesis via a favorable prognostic AS indicator (Fig. 3C). CLK1 had been considered as a novel therapeutic target in GC through phosphoproteomic analysis, and facilitated the proliferation, migration and invasion of GC cells via modulation of the phosphorylation of SRSF2²⁸. The regulatory network in our study also reveals that CLK1 activates the RI event of SRSF2, and generates the spliced variants which favors the prognosis. Interestingly, SRSF2 belongs to the family of SFs itself and contributes to the carcinogenesis of multiple cancers via alternative splicing^{29,30}. Thus, SFs play a pivotal role in tumor development via regulating AS events of key genes.

In conclusion, the present study constructed an ideal prognostic signature of AS events and identified several key regulatory splicing factors, which may provide novel prognostic biomarker and therapeutic target for GC.

Materials And Methods

Data curation and preprocessing

The GC cohort, including RNA-Seq (level 3) and corresponding clinical data were downloaded and integrated via R “TCGAbiolinks” package from TCGA data portal (<https://portal.gdc.cancer.gov/>). The SpliceSeq data for GC were obtained from TCGA SpliceSeq database (<https://bioinformatics.mdanderson.org/TCGASpliceSeq>). The Percent Spliced In (PSI), ranging from 0 to 1, was used in quantifying 7 types of alternative splicing events: Exon Skip (ES), Mutually Exclusive Exons (ME), Retained Intron (RI), Alternate Promoter (AP), Alternate Terminator (AT), Alternate Donor site (AD), and Alternate Acceptor site (AA). For generation of a reliable prognostic model, the included AS events meets the following criterion: (1) more than 75% patients owns PSI value; (2) mean PSI of AS event in all samples > 0.1; (3) PSI standard deviation (SD) ≥ 0.05. In addition, patients followed up for over 30 days were enrolled in our study.

Prognostic model construction via three-step regression analysis

The univariate Cox regression analysis was carried out to screen survival related AS events. To avoid confronting factors, only patients with follow-up time more than 30 days were enrolled in our study. Upset plot was generated to quantify specific overlapping among seven types of AS events with the Upset package in R. Then, stratified by the splicing type, the top 20 significant (If available) AS events screened above were further selected through LASSO regression (R glmnet) followed by multivariate Cox regression (R survival). Finally, the Cox proportional hazard regression model for each splicing type was constructed. The risk score of each sample was calculated by the following formula: Risk Score= PSI of gene1×β1+PSI of gene2×β2+……+ PSI of gene n×βn. Using the median risk score as the cutoff, GC patients were divided into low- and high-risk group. Kaplan-Meier survival analysis with log rank test was performed to demonstrate the variation between these two groups. In addition, the predictive power of each AS signature was evaluated by calculating the Receiver operating characteristic (ROC) area under the curve (AUC).

GO, KEGG and PPI network

Moreover, parent genes of these AS events were sent for Gene Ontology (GO) and Kyoto Encyclopedia of Genes and Genomes (KEGG) enrichment analyses via clusterProfiler package in R. Then, the significantly enriched GO terms and KEGG pathways ($P<0.05$) were visualized via barplot diagrams. Additionally, these parent genes were submitted to STRING to identify the protein-protein interactions (PPIs) which were further visualized with the cytoscape software. The key modules and genes were selected in PPI network via using the Cytohubba tool.

Construction of splicing regulatory Network

A total of 404 human SF genes were retrieved from the Supplementary files of Seiler M`'s paper³¹, and their corresponding expression profiles were extracted from RNA-Seq data. Then, Spearman test was conducted to analyze the correlation between the expression of SF genes and PSI values of survival-associated AS events ($P<0.001$, coefficient>0.6), followed by network plotting using the cytoscape software.

Declarations

Funding

No funding

Competing interests

The authors report no conflicts of interest in this work.

Availability of data and materials

All data are available from the corresponding author on reason-able request.

Ethical approval and consent to participate

Not applicable.

Patient consent for publication

Not applicable.

Authors` contributions

Jingwu Li designed the study. Zhiwu Wang performed the bioinformatics analyses of TCGA and spliceSeq data. Qiong Wu wrote the article. Yankun Liu performed the literature research.

Acknowledgements

The authors would like to acknowledge the staff members in TCGA and spliceSeq database.

References

1. Siegel, R. L., Miller, K. D. & Jemal, A. Cancer statistics, 2020. *CA Cancer J Clin.***70**, 7–30 <https://doi.org/10.3322/caac.21590> (2020).
2. Chen, M. X. *et al.* Phylogenetic comparison of 5' splice site determination in central spliceosomal proteins of the U1-70K gene family, in response to developmental cues and stress conditions. *Plant J.***103**, 357–378 <https://doi.org/10.1111/tpj.14735> (2020).
3. Liang, X. *et al.* PTBP3 contributes to the metastasis of gastric cancer by mediating CAV1 alternative splicing. *Cell Death Dis.***9**, 569 <https://doi.org/10.1038/s41419-018-0608-8> (2018).
4. Zhu, S. *et al.* Regulation of CD44E by DARPP-32-dependent activation of SRp20 splicing factor in gastric tumorigenesis. *Oncogene.***35**, 1847–1856 <https://doi.org/10.1038/onc.2015.250> (2016).
5. Peng, K. *et al.* A 16-mRNA signature optimizes recurrence-free survival prediction of Stages II and III gastric cancer. *J Cell Physiol.***235**, 5777–5786 <https://doi.org/10.1002/jcp.29511> (2020).
6. Yang, Y. *et al.* Genome-wide identification of a novel miRNA-based signature to predict recurrence in patients with gastric cancer. *Mol Oncol.***12**, 2072–2084 <https://doi.org/10.1002/1878-0261.12385> (2018).
7. Wang, Y., Zhang, H. & Wang, J. Discovery of a novel three-long non-coding RNA signature for predicting the prognosis of patients with gastric cancer. *J Gastrointest Oncol.***11**, 760–769 <https://doi.org/10.21037/jgo-20-140> (2020).
8. Zong, Z. *et al.* Genome-Wide Profiling of Prognostic Alternative Splicing Signature in Colorectal Cancer. *Front Oncol.***8**, 537 <https://doi.org/10.3389/fonc.2018.00537> (2018).
9. Zeng, Y. *et al.* Identification of Prognostic Signatures of Alternative Splicing in Glioma. *J Mol Neurosci.***70**, 1484–1492 <https://doi.org/10.1007/s12031-020-01581-0> (2020).

10. Li, S., Hu, Z., Zhao, Y., Huang, S. & He, X. Transcriptome-Wide Analysis Reveals the Landscape of Aberrant Alternative Splicing Events in Liver Cancer. *Hepatology*.**69**, 359–375 <https://doi.org/10.1002/hep.30158> (2019).
11. Zhao, D. *et al.* Survival-associated alternative splicing signatures in non-small cell lung cancer. *Aging (Albany NY)*.**12**, 5878–5893 <https://doi.org/10.18632/aging.102983> (2020).
12. Zhou, Y. J. *et al.* Survival-Associated Alternative Messenger RNA Splicing Signatures in Pancreatic Ductal Adenocarcinoma: A Study Based on RNA-Sequencing Data. *DNA Cell Biol*.**38**, 1207–1222 <https://doi.org/10.1089/dna.2019.4862> (2019).
13. Li, Y. *et al.* Prognostic alternative mRNA splicing signature in non-small cell lung cancer. *Cancer Lett*.**393**, 40–51 <https://doi.org/10.1016/j.canlet.2017.02.016> (2017).
14. Davy, G. *et al.* Detecting splicing patterns in genes involved in hereditary breast and ovarian cancer. *Eur J Hum Genet*.**25**, 1147–1154 <https://doi.org/10.1038/ejhg.2017.116> (2017).
15. Marzese, D. M., Manughian-Peter, A. O., Orozco, J. I. J. & Hoon, D. S. B. Alternative splicing and cancer metastasis: prognostic and therapeutic applications. *Clin Exp Metastasis*.**35**, 393–402 <https://doi.org/10.1007/s10585-018-9905-y> (2018).
16. Martinez-Montiel, N., Rosas-Murrieta, N. H., Anaya Ruiz, M., Monjaraz-Guzman, E. & Martinez-Contreras, R. Alternative Splicing as a Target for Cancer Treatment. *Int J Mol Sci*.**19**, <https://doi.org/10.3390/ijms19020545> (2018).
17. Peng, W. Z., Liu, J. X., Li, C. F., Ma, R. & Jie, J. Z. hnRNPK promotes gastric tumorigenesis through regulating CD44E alternative splicing. *Cancer Cell Int*.**19**, 335 <https://doi.org/10.1186/s12935-019-1020-x> (2019).
18. Li, Y. *et al.* Modification of Mcl-1 alternative splicing induces apoptosis and suppresses tumor proliferation in gastric cancer. *Aging (Albany NY)*.**12**, 19293–19315 <https://doi.org/10.18632/aging.103766> (2020).
19. Li, J. *et al.* Isoforms S and L of MRPL33 from alternative splicing have isoform-specific roles in the chemoresponse to epirubicin in gastric cancer cells via the PI3K/AKT signaling pathway. *Int J Oncol*.**54**, 1591–1600 <https://doi.org/10.3892/ijo.2019.4728> (2019).
20. Liu, C. *et al.* Systematic profiling of alternative splicing in Helicobacter pylori-negative gastric cancer and their clinical significance. *Cancer Cell Int*.**20**, 279 <https://doi.org/10.1186/s12935-020-01368-8> (2020).
21. Armero, V. E. S. *et al.* Transcriptome-wide analysis of alternative RNA splicing events in Epstein-Barr virus-associated gastric carcinomas. *PLoS One*.**12**, e0176880 <https://doi.org/10.1371/journal.pone.0176880> (2017).
22. Zong, Z. *et al.* Integrative bioinformatics analysis of prognostic alternative splicing signatures in gastric cancer. *J Gastrointest Oncol*.**11**, 685–694 <https://doi.org/10.21037/jgo-20-117> (2020).
23. Zhang, S. *et al.* Prognostic significance of survival-associated alternative splicing events in gastric cancer. *Aging (Albany NY)*.**12**, <https://doi.org/10.18632/aging.104013> (2020).

24. Yang, F. *et al.* FBXW2 suppresses migration and invasion of lung cancer cells via promoting β -catenin ubiquitylation and degradation. *Nat Commun.***10**, 1382 <https://doi.org/10.1038/s41467-019-09289-5> (2019).
25. Dvinge, H., Kim, E., Abdel-Wahab, O. & Bradley, R. K. RNA splicing factors as oncoproteins and tumour suppressors. *Nat Rev Cancer.***16**, 413–430 <https://doi.org/10.1038/nrc.2016.51> (2016).
26. Bejar, R. Splicing Factor Mutations in Cancer. *Adv Exp Med Biol.***907**, 215–228 https://doi.org/10.1007/978-3-319-29073-7_9 (2016).
27. Li, F. *et al.* QKI5-mediated alternative splicing of the histone variant macroH2A1 regulates gastric carcinogenesis. *Oncotarget.***7**, 32821–32834 <https://doi.org/10.18632/oncotarget.8739> (2016).
28. Babu, N. *et al.* Phosphoproteomic analysis identifies CLK1 as a novel therapeutic target in gastric cancer. *Gastric Cancer.***23**, 796–810 <https://doi.org/10.1007/s10120-020-01062-8> (2020).
29. Luo, C. *et al.* SRSF2 Regulates Alternative Splicing to Drive Hepatocellular Carcinoma Development. *Cancer Res.***77**, 1168–1178 <https://doi.org/10.1158/0008-5472.Can-16-1919> (2017).
30. Liang, Y. *et al.* SRSF2 mutations drive oncogenesis by activating a global program of aberrant alternative splicing in hematopoietic cells. *Leukemia.***32**, 2659–2671 <https://doi.org/10.1038/s41375-018-0152-7> (2018).
31. Seiler, M. *et al.* Somatic Mutational Landscape of Splicing Factor Genes and Their Functional Consequences across 33 Cancer Types. *Cell Rep.***23**, 282–296284 <https://doi.org/10.1016/j.celrep.2018.01.088> (2018).

Figures

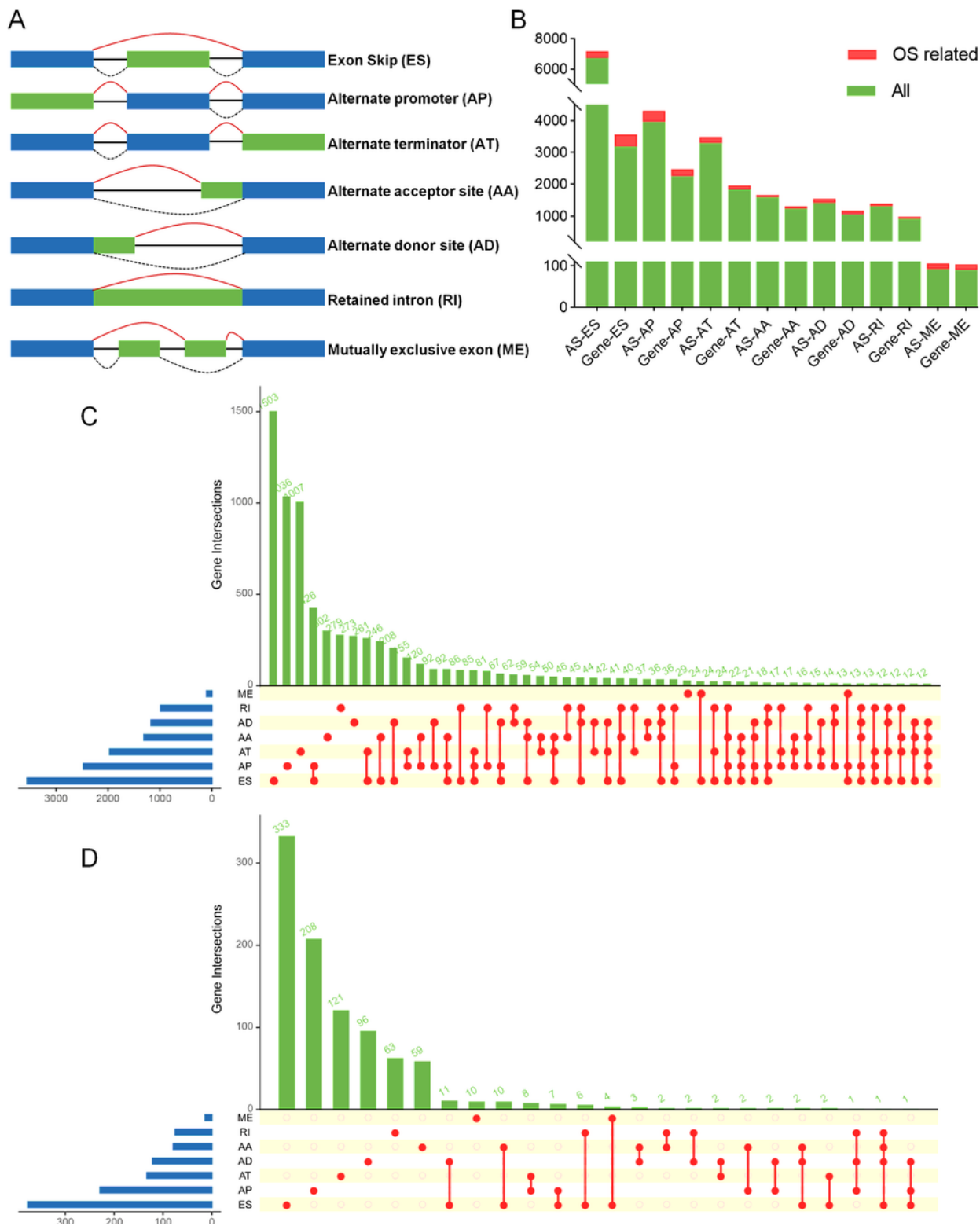


Figure 1

Overview of AS profiles in GC cohort. (A), Depiction for 7 splicing patterns, including Exon Skip (ES), Alternate Promoter (AP), Alternate Terminator (AT), Alternate Donor Site (AD), Alternate Acceptor Site (AA), Mutually Exclusive Exon (ME) and Retained Intron (RI). (B), Number of AS events and related genes. The green bars represent all AS events and parent genes, the red bars represent survival related AS events and

parent genes. (C), Upset plot of interactions within 7 types of all AS events. (D), Upset plot of interactions within 7 types of prognosis related AS events.

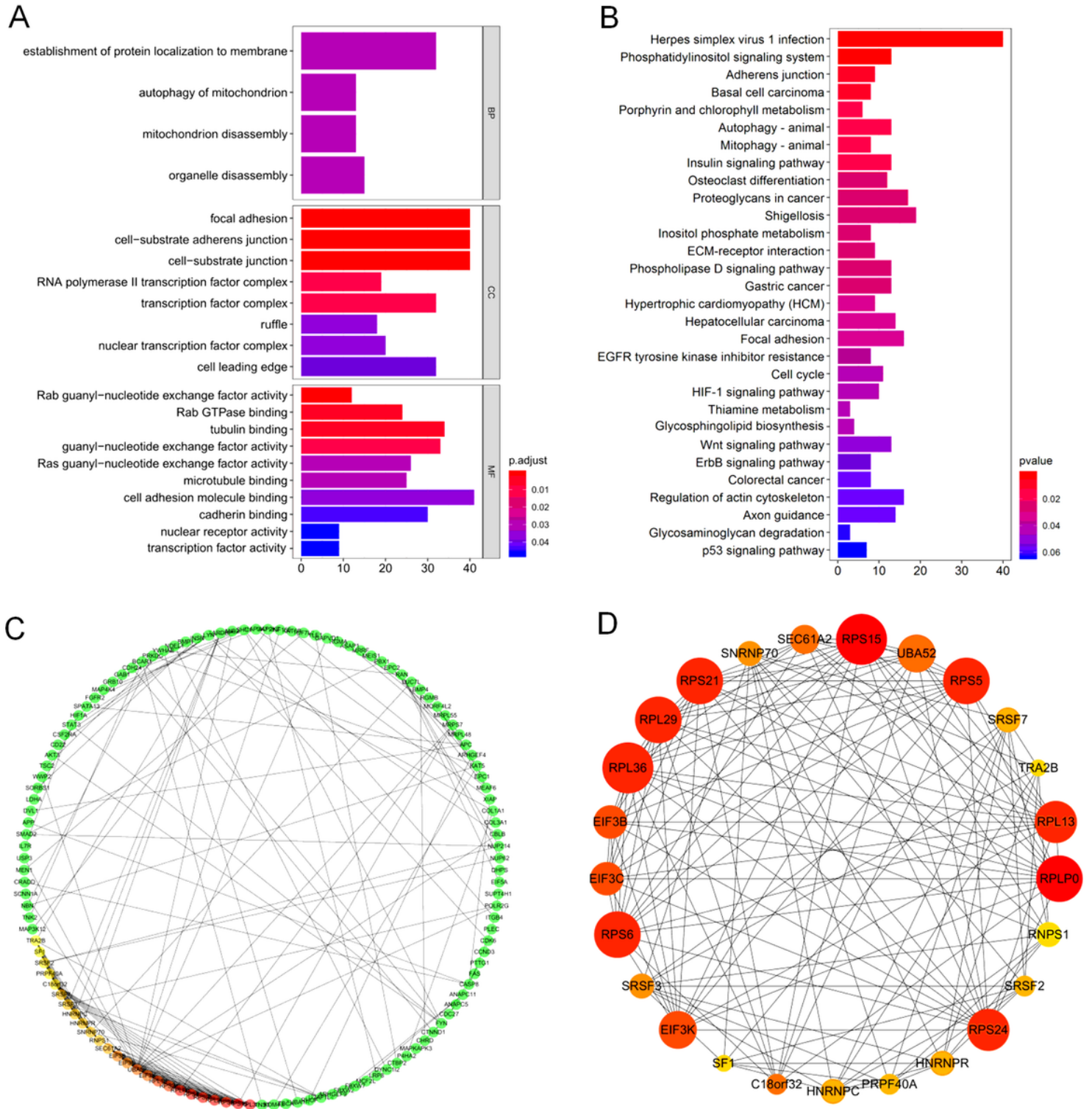


Figure 2

Enrichment analyses on parent genes from Overall survival (OS) related AS events and their interacting network. (A), Top 10 items (If available) of GO in Biological process (BP), Cellular component (CC) and Molecular function (MF). (B), Top 30 pathways in KEGG. (C), Protein Protein Interaction (PPI) network on

parent genes of OS related AS events. (D), The core module derived from the PPI network. The node size represents the connectivity to other agents. The larger the node in size, the more important the node.

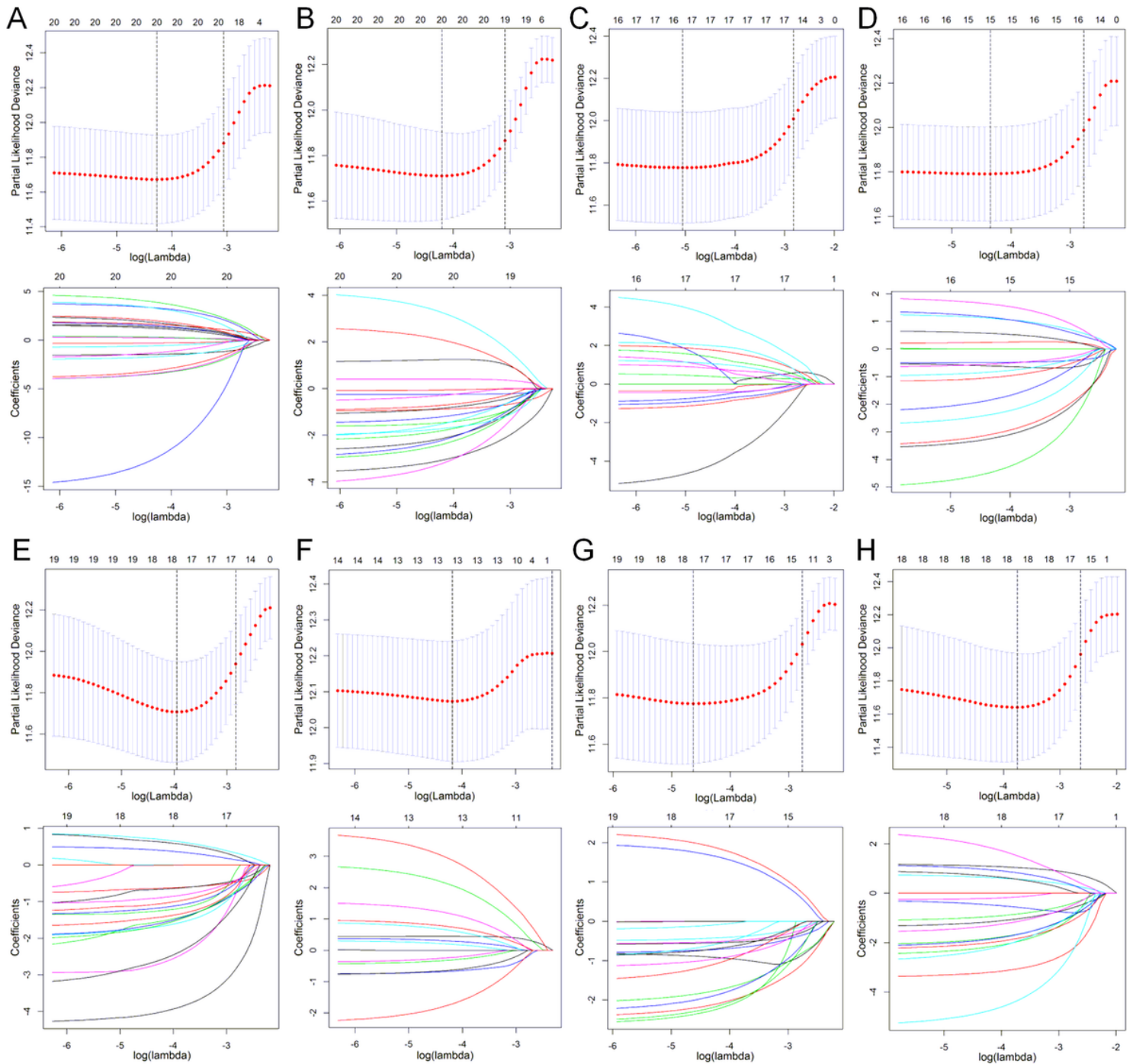


Figure 3

Lasso regression analysis of OS related AS events by AA, AD, AP, AT, ES, ME, RI type (A-G) and all types (H). Upper, selection of tuning parameter (lambda) in Cox penalized regression analysis via 10-fold cross validation. The vertical dotted line on the left and right represents the “lambda.min” and “lambda.lse” criteria, respectively. Lower, dynamic lasso coefficient profiling by Cox-penalized model.

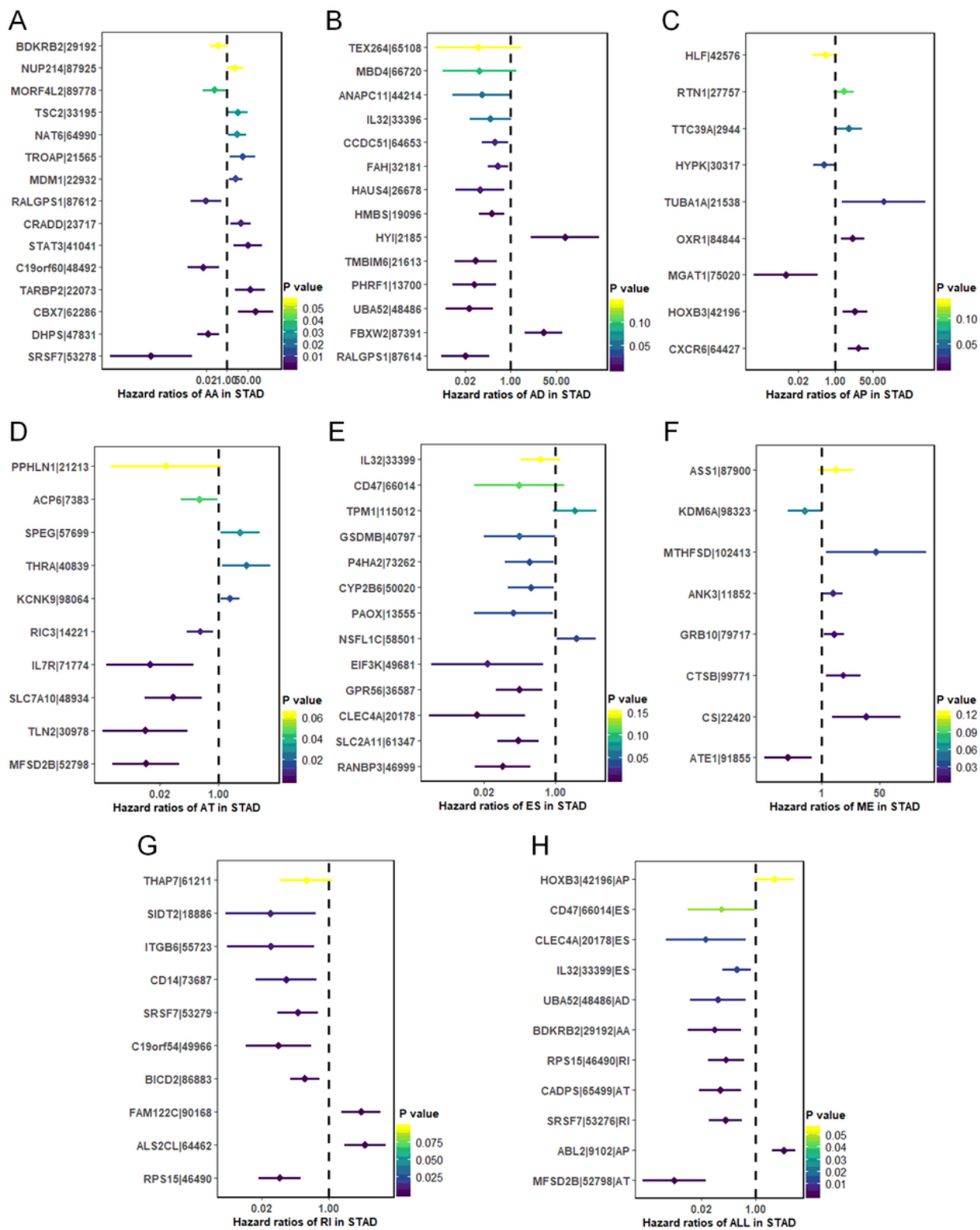


Figure 4

Forest plots of OS related AS events via Multivariate Cox regression according to stratified (A-G: AA, AD, AP, AT, ES, ME, RI) or non-stratified (H) strategy. Hazard ratios and 95% Confidence intervals of Overall survival (OS) related AS events

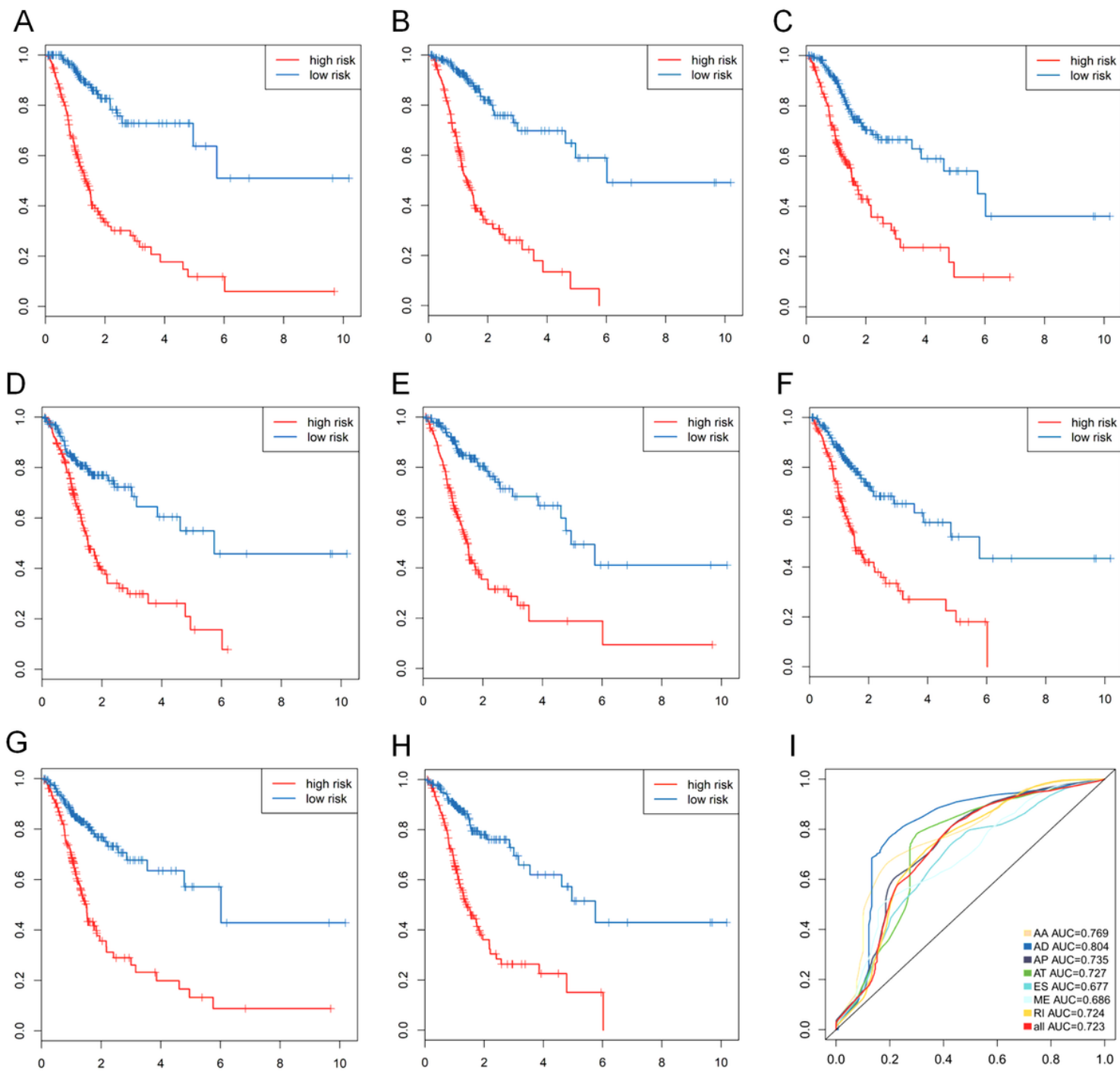


Figure 5

Kaplan-Meier and ROC curves of prediction models in GC. (A-H), Kaplan-Meier curves depicting the survival probability between high (red)- and low (blue)-risk score groups calculated by AA, AD, AP, AT, ES, ME, RI type and all types. (I), ROC curve for AA, AA, AD, AP, AT, ES, ME, RI type and all types.

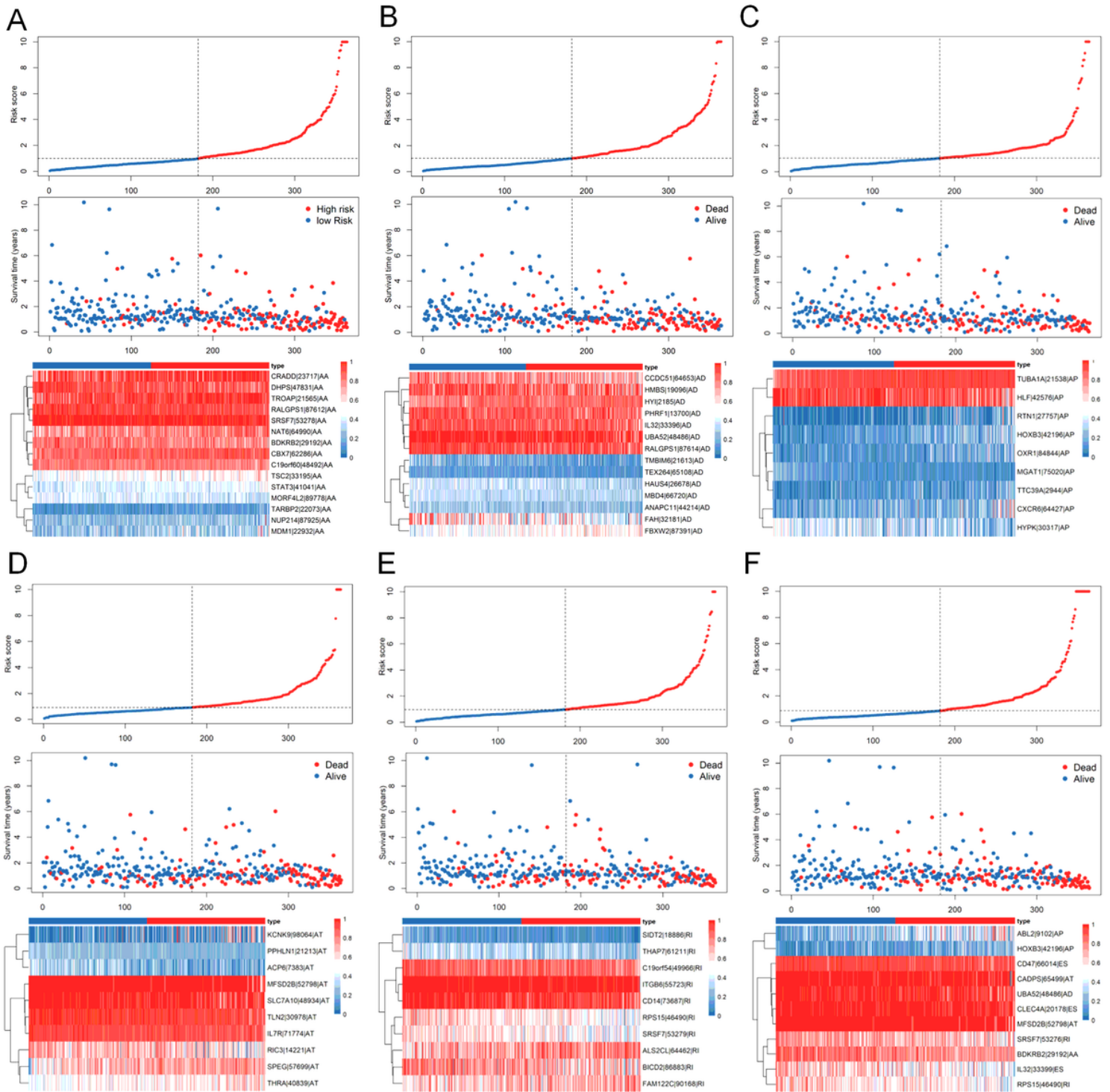


Figure 6

Distributions of survival status (Up), risk score (Middle) and expression profile (Down) of the most reliable prognostic signatures with AUC>0.7. (A), AD type; (B), AA type; (C), AP type; (D), AT type; (E), RI type; (F), non-stratified by the splicing type.

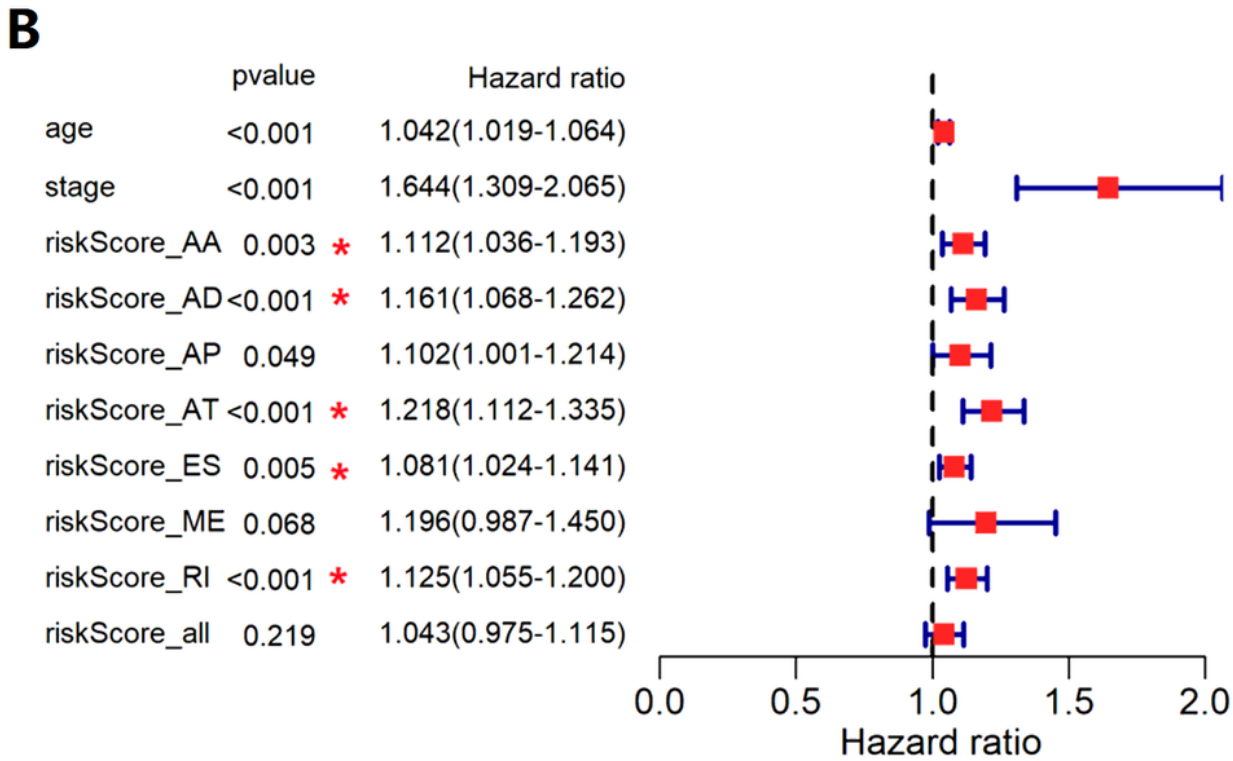
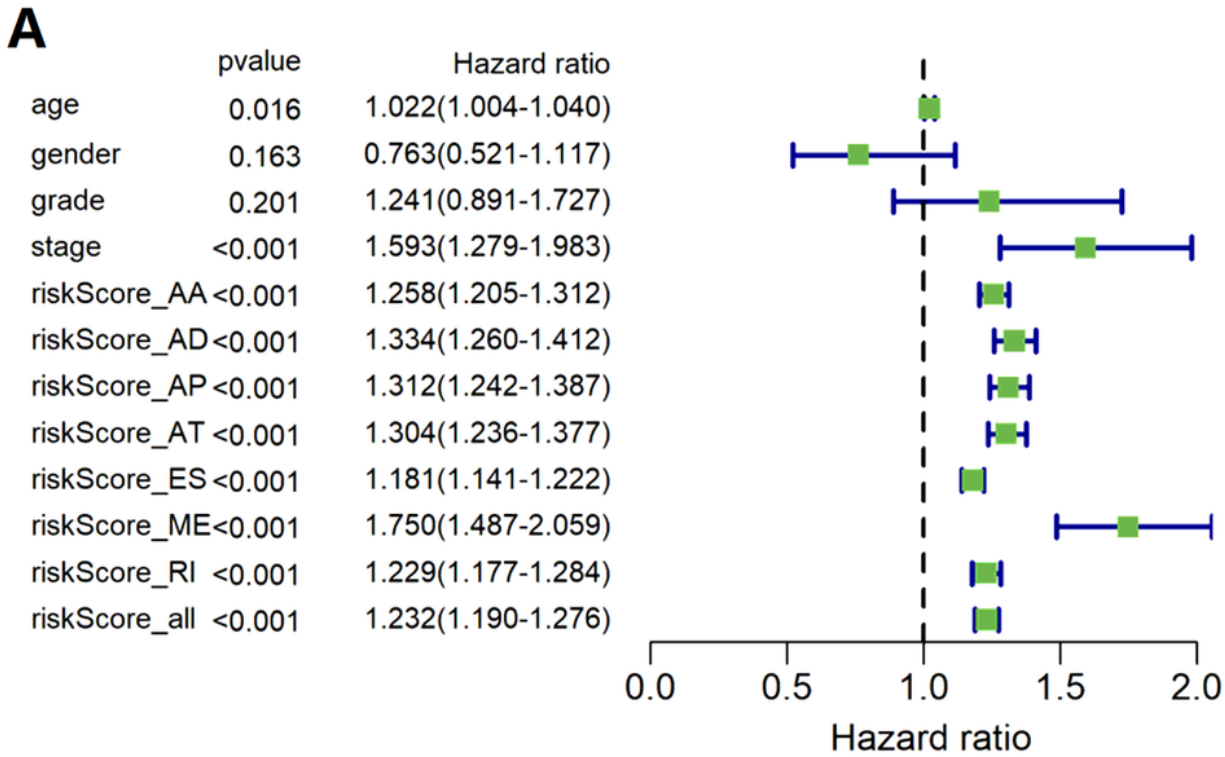


Figure 7

Forest plots of univariate (A) and multivariate (B) analyses of AS types combined with age, gender, grade and stage.

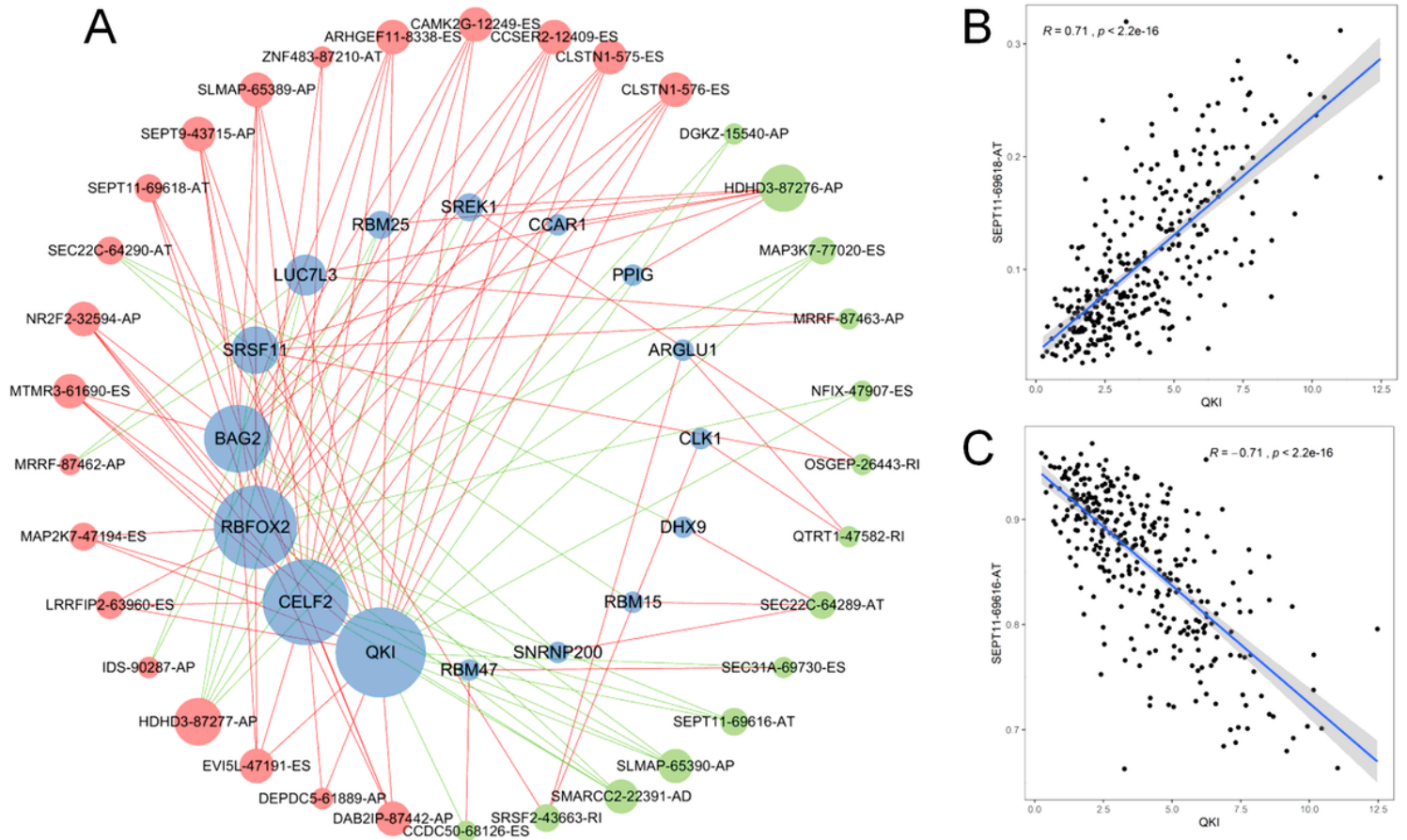


Figure 8

The regulatory network of splicing factor and parent genes in GC. (A), the network of SF expression and PSI value of AS genes. Red, green and blue node represents adverse, favorable AS events and SF, respectively. (B-C), The correlation plot of SF QKI and PSI value of SEPT11-69616-AT, SEPT11-69618-AT, respectively.